Land-Surface parameters and objects in hydrology

Gruber, S ; Peckham, S

DOI: https://doi.org/10.1016/S0166-2481(08)00007-X

CHAPTER 7

Land-Surface Parameters and Objects in Hydrology

S. Gruber and **S. Peckham**

phenomena related to the flow of water or other materials that can be parameterised using a DEM · basic principles and approaches to modelling of flow · differences between the diverse flow-modelling techniques available · advantages, disadvantages and limitations of the different approaches · why is parameterisation of surface flow a powerful technique?

1. HYDROLOGICAL MODELLING

Hydrology is the study of the movement, distribution, and quality of water throughout the Earth. The movement of water is primarily driven by gravity and to some degree modified by the properties of the material it flows through or flows over. The effect of gravity can mostly be approximated well and easily with a DEM. By contrast, surface and subsurface properties and conditions are rather cumbersome to gather and to treat. From this simple reasoning it is also evident, that in steep topography such parametrisation performs better than in very gentle topography where the relative importance of gravity decreases. Parametrisation means that we represent certain phenomena related to the flow of water with quantities (parameters) that are easy to calculate and/or for which data are readily available. In many cases we can deduce much information from the DEM, alone. However, one needs to be careful not to stretch these methods to applications that suffer from the inherent simplifications.

Land-surface parameters specific to hydrology have been applied to a multitude of different areas including:

- hydrological applications (Chapter 25);
- mapping of landforms and soils (Chapter 20);
- modelling landslides and associated hazard (Claessens et al., 2005);
- hazard mapping (ice/rock avalanches, debris flows) in steep terrain (Chapter 23);

Developments in Soil Science, Volume 33 © 2009 Elsevier B.V.
ISSN 0166-2481, DOI: 10.1016/S0166-2481(08)00007-X.

- erosion and deposition modelling (Mitášová et al., 1996);
- mass balance modelling on mountain glaciers (Machguth et al., 2006).

Most of these applications focus on steep terrain (hill slopes and headwaters), where topography clearly dominates the flow of water. Many hydrologic applications, however, also involve nearly horizontal terrain (channels and flood plains of large rivers) and require specific techniques to produce consistent results in areas where the flow of water is governed by features that are smaller than the resolution or uncertainty of the DEM.

The development and use of flow-based land-surface parameters gained importance in the late 1980s after the introduction of the D8 algorithm (O'Callaghan and Mark, 1984) and the 1990s have seen a number of multiple flow directions algorithms published and employed (Freeman, 1991; Quinn et al., 1991; Holmgren, 1994). Similarly, corresponding techniques for the treatment of ambiguous flow directions (Garbrecht and Martz, 1997) or the derivation of hydrologically-sound DEMs (Hutchinson, 1989) as well as sensitivity studies using existing algorithms (Wolock and Mccabe, 1995) were published. Methods based on original contour data (O'Loughlin, 1986) and TINs (Jones et al., 1990; Tucker et al., 2001) have some advantages over using gridded DEMs but have continued to play a subordinate role due to the wide availability and intuitive processing of raster data as well as the introduction of more advanced techniques for extracting information from raster DEMs.

While the development and refinement of methods is still ongoing, the near future will likely see much research dedicated to the optimal use of high-resolution and high-quality LiDAR elevation data sets that are currently becoming widely available.

2. FLOW DIRECTION AND ASPECT

2.1 Understanding the idea of flow directions

Flow direction is the most basic hydrology-related parameter and it forms the basis for all other parameters discussed in this chapter. Imagine you are standing somewhere in a hilly landscape that has a smooth ground surface. If you release one drop of ink on the ground, you intuitively expect it to flow down the steepest path at each place and to leave a trace on the ground that represents what is called a *flow line*. The physics of purely gravity-driven flow dictates that water will always take the steepest downhill path, such that flow lines cross contour lines at a right angle.

However, when we imagine a grid cell centred on a peak or *ridge line*, the flow direction is ambiguous, no matter how small we make the cell. In fact, flow direction for peaks and ridges is ambiguous even for mathematical surfaces with infinite resolution. Consistent flow distribution demands flow into opposite directions and thus violates the notion of having only one flow line or direction for each grid cell. In sloping terrain, such ambiguous flow directions are always *sub-grid* effects that cannot be represented at the present resolution. If, however, the surface

is discretised (e.g. into a regular grid), then we are faced with the problem of how best to represent a continuous flow field with a regular grid. Then, the number of neighbouring directions that a drop can move to is limited and the best compromise needs to be found. This is the first problem of assigning one *single flow direction* to each grid cell in a regular grid that only has eight possible directions in multiples of 45° (Figure 1).

The second problem relates to the *divergence* (going-apart) — the opposite being *convergence* (coming-together) — of flow. If you release two drops on an inclined plane, they will keep flowing down slope, parallel to each other with constant spacing between their traces (flow lines). On the surface of a cone (plan-convex, see Section 2.1 in Chapter 6), the drops increase their spacing as they flow down slope — their flow lines are divergent. This means that there is the same mass (e.g. number of drops or volume of water) spread over a larger area. Similarly, on an inverted cone (plan-concave), two drops that are released nearby decrease their spacing — their tracks are convergent.

This entire section mainly deals with the formulation of how to move how much water into which neighbouring cells in order to have a representation of reality that is suitable for a given task. This can be pictured as many drops flowing from one cell to one or more adjacent cells, depending on their relative elevations. The partitioning of mass (or number of drops) contained in one cell to several lower neighbours may be justified by actual divergence or by the attempt to overcome the limits of having only 8 adjacent cells. If the local direction of steepest decent is not a multiple of 45°, then the flow may be partitioned between two neighbours to account for this. As a consequence, the water of one cell may be propagated into *multiple neighbour cells*.

However, the initial mass is then contained in two or more cells instead of one and thus dispersed over a larger area and a larger width along the contours. For some applications this may be inappropriate and is then termed over-dispersal. Now, we have assembled all four criteria by which to judge or select a flow direction algorithm:

(1) *handling of the discretization* into only eight possible adjacent flow directions (artifacts are sometimes called *grid bias*);
(2) *handling of divergence*;
(3) *handling of dispersal*; and
(4) *handling of sub-grid effects*.

At the same time it is evident that all four criteria are interconnected and that each algorithm will be a compromise between them. Often two more criteria are mentioned that we will not discuss in detail here but that can be very important for certain applications. One is the suitability for efficient computational evaluation and the other is the robustness of the method (i.e. its ability to describe all terrain shapes without exceptions). The basic types of *single- and multiple-neighbour flow algorithms* are fundamentally different: single-neighbour algorithms cannot represent divergent flow but for the same reason have no problem of over-dispersal. Multiple-neighbour algorithms can represent divergent flow but usually also suffer from some over-dispersal. Flow direction is ambiguous on peaks and ridges,

which occur throughout fluvial landscapes and which are essentially singularities in the flow field.

2.2 Handling undefined flow directions

The assignment of flow directions relies on elevation difference between cells to drive the flow. This principle fails for local elevation minima (*pits*) that have no lower neighbours and for horizontal areas. Thus, an undefined drainage direction is often assigned to pits (no drainage direction) and horizontal areas (ambiguous or no drainage direction) resulting in the termination of flow accumulation in such cells. This effect may be:

- *real and wanted* (e.g. sinkholes in Karst);
- *real but unwanted* (e.g. if flow accumulation is desired to propagate though a lake);
- *artificial and unwanted* (e.g. pit artifacts in a DEM or falsely horizontal areas in large river plains).

If these effects are unwanted (in most cases they are), alternative methods[1] have to be employed for the designation of a flow direction in order to keep the physical quantities of derived land-surface parameters consistent. Horizontal areas are rare in real landscapes but can exist in DEMs where a cell is usually considered horizontal if it has the same elevation as its lowermost neighbour. Horizontal areas can originate from lakes, from interpolation artifacts or be the result of preprocessing during which depression have been filled. *Large rivers* also have very low slopes that usually are smaller than the DEM resolution and thus locally appear to be horizontal.

> REMARK 1. *In large river basins, special techniques can be required to calculate channel slope that is often lower than can be represented by the DEM.*

One approach to resolve ambiguous flow direction in flat areas is an iteration procedure during which flat cells are assigned a single flow direction to a draining neighbour cell (Jenson and Domingue, 1988) and the actual elevation values remain unchanged. In the first iteration this will only make cells next to outlets drain. In the second iteration, flat calls adjacent to the ones altered during the first step will receive a flow direction and so on. This approach has been extended to avoid unrealistic *parallel drainage lines* (Tribe, 1992a). The second approach is to make minute alterations to the elevation (Garbrecht and Martz, 1997) of the flat cell in order to impose a small artificial gradient (thus often called imposed gradient method). These artificial changes are made in an iterative way and result in topography that is also suitable for flow direction resolution by multiple-neighbour flow methods. However, in many cases this requires an increased numerical resolution of the DEM in computer memory and is often impractical for large river basins.

[1] A number of methods for the treatment of pits is discussed in Section 2.8 of Chapter 4.

2.3 Stream burning

Poor quality or simply the inherent generalisation of a DEM may cause drainage lines derived by digital delineation from gridded data to substantially differ from reality. Where vector hydrography information exists it can be integrated into the DEM prior to the actual analysis. This process is referred to as *stream burning* and can be effective in the digital reproduction of a known and generally accepted stream network. However, it has the disadvantage of locally altering topography in order to provide consistency between existing vector hydrography and the DEM. Several methods exist[2] (Hutchinson, 1989; Saunders and Maidment, 1996) but greatly differ in their success of improving, e.g. watershed delineation (Saunders, 1999). The pre-processing of the vector information required often represents an intensive effort.

2.4 Vertical resolution of DEMs and computation of slope

The above paragraph has discussed the assignment of drainage direction for areas that are horizontal in the DEM. Many times, these areas are not horizontal in reality. This section deals with the problem of assigning a slope to them because it is a key variable in many types of process-based hydrologic models. In the context of flow routing, for example, slope, water depth and roughness height are the main variables that determine the flow velocity. Here we will define slope as a dimensionless ratio of lengths (rise over run) or as the tangent of the slope angle ($\tan \beta$). When working with raster DEMs and computing slopes between grid cells, the ratio of the vertical and horizontal resolutions determines the minimum non-zero slope that can be resolved.

For example, a DEM with a vertical resolution of 1 m and a grid spacing of 30 m has a minimum resolvable slope of $1/30 = 0.0333$, while a DEM with a vertical resolution of 1 cm and a grid spacing of 10 m has a minimum resolvable slope of $1/1000 = 0.001$. This lower bound means that slopes on hillsides can usually be computed with a relatively small error, using any of several different local methods (as discussed in Section 3.3 of Chapter 2). However, slopes in channels are often much smaller than the numbers in these examples, and can even be smaller than 0.00001 for larger rivers. This is several orders of magnitude smaller than can typically be resolved and, as a consequence, these areas will appear horizontal in the DEM and require techniques for flow routing in horizontal areas.

One way to get better estimates of channel slope is to use the flow directions assigned to the horizontal DEM cells (see previous section) to identify a streamline or reach that spans a number of grid cells. The slope can then be computed as the elevation drop between the ends of the reach divided by its along-channel length. Depending on the size of the grid cells, this may yield an estimate of the valley slope instead of the channel slope. Channel sinuosity within the valley bottom will result in an even smaller slope.

[2] See also the AGREE — DEM surface reconditioning system (http://www.ce.utexas.edu/prof/maidment/gishydro/ferdi/); courtesy of Ferdi Hellweger.

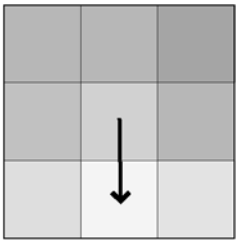

FIGURE 1 Single flow direction assigned to the central pixel in a 3×3 neighbourhood. Grey values represent elevation increasing with darkness of the cell.

3. FLOW ALGORITHMS

3.1 Single-neighbour flow algorithms

The most basic flow algorithm is the so-called "*D8*", sometimes referred to as *method of the steepest descent* (O'Callaghan and Mark, 1984). From each cell, all flow is passed to the neighbour with the steepest downslope gradient (Figure 1) resulting in 8 possible drainage directions — hence the name D8. It can model convergence (several cells draining into one), but not divergence (one cell draining into several cells). Ambiguous flow directions (the same minimum downslope gradient is found in two cells) are usually resolved by an arbitrary assignment.

This method actually provides a very good estimate of the catchment area for grid cells that are far enough downstream to be in the fully convergent, channelised portion of the landscape. However, for grid cells on hillslopes or near peaks and divides where the flow is divergent, values obtained by this method can be off by orders of magnitude. The D8 method is widely used and implemented in many GIS software packages. Despite its limitations, it is useful for a number of applications such as extracting river network maps, longitudinal profiles and basin boundaries.

A number of other single-neighbour algorithms have been published. *Rho8* (Fairfield and Leymarie, 1991) is a stochastic extension of D8 in which a degree of randomness is introduced into the assignment of flow directions in order to reduce the grid bias. The drawback of this method is that — especially for small catchments — it produces different results if applied several times. The aspect-driven *kinematic routing algorithm*[3] (Lea, 1992) specifies flow direction continuously and assigns flow to cardinal cells in a way that traces longer flow lines with less grid bias than D8.

3.2 Multiple-neighbour flow algorithms

Only multiple-neighbour flow methods can accommodate the effects of divergent flow (spreading from one cell to several downhill cells, Figure 2) that are especially important on hill slopes. Four important multiple-neighbour flow algorithms as

[3] Also referred to as "*Lea's method or kinematic routing*".

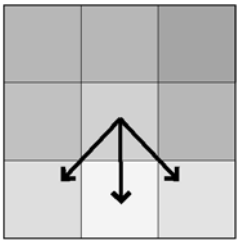

FIGURE 2 Multiple flow directions assigned to the central pixel in a 3×3 neighbourhood using MFD. Grey values represent elevation increasing with darkness of the cell. Multiple flow directions are assigned and a fraction of the mass of the central cell is distributed to each of the three lower cells that the arrows point to. All mass fractions together must sum to one in order to conserve mass.

well as the basic principles of their calculation are described here. This description is intended to highlight the important differences that exist between these approaches and thus help to judge their suitability for a given task.

> REMARK 2. *All flow-routing methods discussed in this chapter can represent convergent flow but only multiple-neighbour methods can accommodate divergent flow.*

3.2.1 Multiple Flow Direction (MFD) Method

A number of algorithms exist that handle divergent flow and partition the flow out of one cell to *all* lower neighbours (Freeman, 1991; Quinn et al., 1991, 1995; Holmgren, 1994). These algorithms do not have firmly-established names and are often simply referred to as MFD (multiple flow direction) methods, as the *TOPMODEL approach* (Quinn et al., 1991) or as *FD8* (Freeman, 1991). In a general formulation, the draining fraction d into neighbouring cell NBi is given by:

$$d_{\mathrm{NB}i} = \frac{\tan(\beta_{\mathrm{NB}i})^v \cdot L_{\mathrm{NB}i}}{\sum_{j=1}^{8}(\tan(\beta_{\mathrm{NB}j})^v \cdot L_{\mathrm{NB}j})} \tag{3.1}$$

The draining fraction d depends on the slope β (positive into lower cells and 0 for higher cells) into the neighbours, on different draining contour lengths L as well as an exponent v controlling dispersion. The drainage potentials into each neighbour are normalised to unity over the 3×3 kernel in order to preserve mass. In this way, different weights can be assigned to downstream pixels between which the flow is partitioned.

High values of v concentrate flow more toward the steepest descent and low values result in stronger dispersion (v must be $\geqslant 0$). Holmgren (1994) suggests values of $v = 4$–6 and equal L for cardinal and diagonal directions to produce best[4] results. In the widely used original TOPMODEL approach (Quinn et al., 1991), no exponent is used to control dispersion ($v = 1$), but differing contour lengths L are

[4] Freeman (1991) suggests $v = 1.1$, but it is unclear if he refers to slope in degrees or as the tangent so this has to be treated with care.

assumed somewhat arbitrarily for cardinal (0.50 × cell size) and diagonal neighbouring pixels (0.35 × cell size). The use of the exponent v makes this method very flexible, but, at the same time it is difficult to determine optimal values for it.

> REMARK 3. *The exponent in multiple flow direction methods only controls the amount but not the area of dispersion.*

Furthermore, it needs to be kept in mind that the exponent v only controls the amount of dispersion (how much volume is passed to each cell) but not the degree of dispersion (to which cells flow is propagated). Minute amounts (only limited by numerical precision) of flow will always be passed to each lower neighbour. A technique to restrict the lateral spreading in MFD methods is presented in Chapter 23.

MFD methods are powerful in handling sub-grid effects: a horizontal ridge pixel for instance will drain towards opposite sides. However, a well-known problem with this method, as pointed out by Costa-Cabral and Burges (1994), Tarboton (1997) and others, is that it produces over-dispersion. That is, this method causes flow to spread too much, with some fraction nearly flowing along the contours. For example, in the case of an inverted cone, some of the flow from a grid cell will eventually make its way to the opposite side of the cone.

3.2.2 D∞

In this approach proposed by Tarboton (1997) one draining flow direction is assigned to each cell. It is continuous between 0 and 2π radians and the *infinite* number of directions that can be assigned is reflected in the name D-Infinity or D∞. (In practice it is beneficial to handle drainage direction in degrees instead of radians to avoid truncation errors in the numerical representation of π leading to small errors in flow routing.) Based on this direction, the draining proportion d is then apportioned (applied to the discrete DEM grid, Figure 3) to the two pixels on either side of the theoretical drainage direction vector by:

$$d_1 = \frac{4 \cdot \alpha_2}{\pi}, \qquad d_2 = \frac{4 \cdot \alpha_1}{\pi} \tag{3.2}$$

The angles α are measured on a horizontal planar surface between the drainage direction vector and the vectors to the two pixels on either side of it ($\alpha_1 + \alpha_2 = 45°$).

The flow is thus partitioned between only two cells and the grid bias inherent in D8 as well as the over-dispersion to all lower neighbours inherent in MFD are avoided. The angle-weighted partitioning however is somewhat arbitrary. The derivation of the flow direction is based on planes defined by the eight point-triplets given by the centre pixels and two adjacent neighbour pixels (for details see Tarboton, 1997). The use of point triplets also avoids the problems associated to the local fitting of planes through four points as employed in the kinematic routing algorithm (Lea, 1992) and DEMON (Costa-Cabral and Burges, 1994). In situations of ambiguous drainage direction this approach assigns one direction arbitrarily. Drainage towards two sides (horizontal ridge) is therefore impossible.

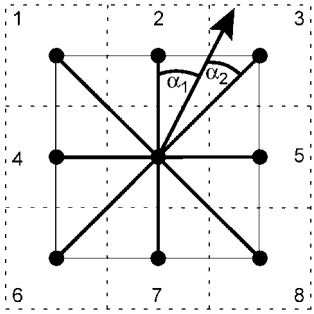

FIGURE 3 Concept of flow apportioning in D∞ (following Tarboton, 1997). A 3×3 pixel neighbourhood is given by the dashed lines and margin pixels are numbered 1 to 8. Pixel centres are represented by black points. The thick lines connecting the centres form eight triangles over which the drainage direction vector (arrow) is determined. Using this drainage direction vector, the flow is apportioned to the two pixels that bound the facet that the vector lies on. In this case, flow is distributed between pixels 2 and 3 [see Equation (3.2) where the subscripts 1 and 2 refer to pixels 2 and 3 in this example].

3.2.3 DEMON

This method relies on the construction of flow tubes based on best-fit planes through the four corners of a pixel and generally produces very realistic results in both convergent and divergent flow regimes (Costa-Cabral and Burges, 1994). However, the method that is used to determine aspect angle can lead to inconsistent flow geometry and does not address the ambiguity of flow direction on peaks and ridges. This method is implemented in only few software packages.

3.2.4 Mass-Flux Method (MFM)

The second author (S. Peckham) has developed another method called the Mass-Flux Method which is available in RiverTools (see Chapter 18). This method has so far not been published and evaluated in the scientific literature but both the promising results of its application as well as its basic concept warrant a brief description, here. The key idea of this method is to divide each grid cell into four *quarter pixels* and to define a continuous flow direction angle for each, using a grid that has twice the dimensions of the DEM. For each quarter pixel, the elevations of the *whole pixel* and two of its cardinal neighbours uniquely determine a plane and a corresponding slope and aspect (Figure 4).

While this removes the ambiguity of plane fitting and the associated problems, it also removes the ambiguity of flow direction for grid cells that correspond to peaks or ridges, since it allows flow from these grid cells to be routed in different directions. At the quarter-pixel scale, however, flow from each quarter pixel is only permitted to flow into one or two of its cardinal neighbours. The fraction that flows into these neighbours is determined by treating each grid cell as a control volume. Flow out of a control volume can only be through an edge. There can be no flow directly to a diagonal neighbour. The fraction of flow that passes through a given edge is computed as the dot product of the unit normal vector for that edge

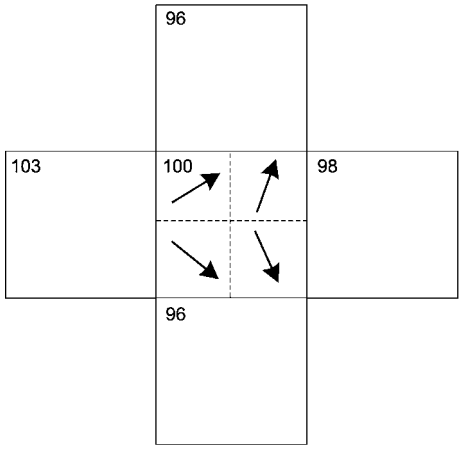

FIGURE 4 Flow directions assigned to quarter pixels using the Mass-Flux Method. Numbers refer to pixel elevations in this example. © 2005 Rivix LLC, used with permission.

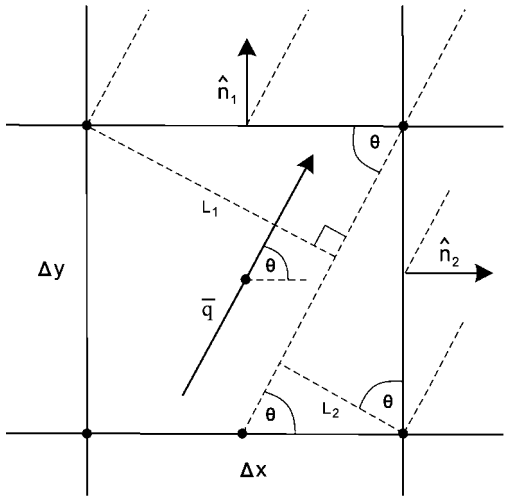

FIGURE 5 Flow apportioning between two cardinal neighbours in the Mass-Flux Method. L_1 and L_2 denote the projected flow widths into the upper and left neighbour and together equal the projected flow width w, $\hat{n}_1$ and $\hat{n}_2$ are vectors normal to the cell boundaries, $\bar{q}$ is the flow vector and θ is the flow direction. © 2005 Rivix LLC, used with permission.

and the continuous-angle flow vector, as shown in Figure 5. This is equivalent to decomposing the flow vector into two vector components along the grid axes.

Where flow is convergent, it is possible for two quarter-pixels to have a component of flow toward each other. This occurs because streamlines in the actual flow field are closer together than the grid spacing. While we know that streamlines cannot cross, the additional turning required for the streamlines to become paral-

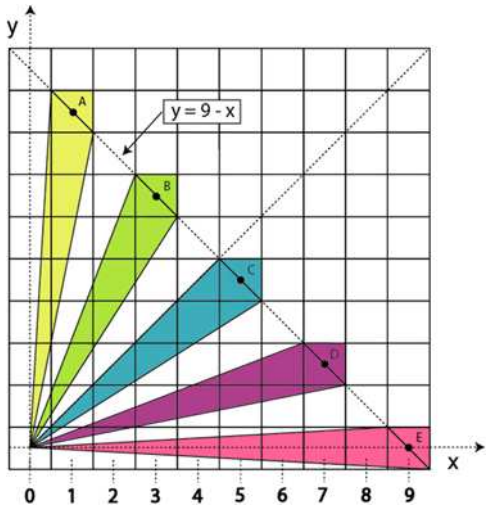

FIGURE 6 For the special case of a radially-symmetric surface such as a cone or a Gaussian hill, the TCA for pixels can be computed analytically. Each"*necktie*" region can be broken into two triangles of which the area can be computed. This shows that pixels A–E each have the same TCA. In this regular case ($\Delta x = \Delta y$), the flow width can thus vary between 1 and $\sqrt{2}$ multiplied by the grid resolution. © 2005 Rivix LLC, used with permission.

lel cannot be resolved. To address this streamline resolution problem, the grid of quarter-pixel aspect angles is scanned for these cases prior to computing the total contributing area (see below) and the angles are adjusted by the smallest amount that is necessary to produce a consistent vector field.

A grid of total contributing area values with the same dimensions as the DEM is found by integrating the contributions of the eight quarter-pixels that surround each whole pixel. Similarly, a whole-pixel grid of aspect angles is found using the vector sum of the quarter-pixel flow vectors.

3.3 Flow width

The flow width or effective contour length orthogonal to the outflow (w) is another important concept in hydrology and for flow-based parameters. For the D8 and MFD methods, flow widths to each of the eight neighbours must be defined in some manner, and a variety of different rules have been proposed. In the TOPMODEL approach (Quinn et al., 1991), different contour length factors (cardinal: $0.50 \times \Delta x$, diagonal: $0.35 \times \Delta x$) are accumulated over all draining directions. For multiple-neighbour methods that use a single, continuous flow angle such as Lea (1992) method, D-Infinity, DEMON and the Mass-Flux Method, the projected pixel width (Figures 5 and 6) can be computed as:

$$w = \left|\sin(\theta)\right| \cdot \Delta x + \left|\cos(\theta)\right| \cdot \Delta y \tag{3.3}$$

where θ is the aspect angle, and Δx and Δy are the grid cell sizes[5] along the two coordinate axes.

4. CONTRIBUTING AREA/FLOW ACCUMULATION

The concept of *contributing area* is very important for hydrologic applications since it determines the size of the region over which water from rainfall, snowfall, etc. can be aggregated. It is well known that the contributing area of a watershed is highly correlated with both its mean-annual and peak discharge. The *dendritic* nature of river networks results in water collected over a large area being focused to flow in a relatively narrow channel. Contributing area, also known as *basin area*, *upslope area* or *flow accumulation* is a planar area and not a surface area. It describes the spatial extent of a collecting area as seen from the sky.

When we speak of *Total Contributing Area* (TCA), we have an element of finite width in mind such as a grid cell or contour line segment and we are integrating the flow over this width. *Specific Contributing Area* (SCA) refers to area per unit contour length (SCA = TCA/w), and is the more fundamental quantity that must be integrated over some width to get the TCA. This distinction is analogous to how the terms discharge and specific discharge are used. In fact, in the idealised case of constant, spatially uniform rainfall rate, the TCA and SCA are directly proportional to the discharge and specific discharge. This correspondence makes it possible to recast the problem of computing contributing area as a steady-state flow problem.

Flow accumulation cannot only be used to accumulate contributing area but also other quantities such as the amount of contributing pixels, accumulated precipitation (spatially-varying input) or *accumulated terrain attributes* (e.g. elevation) that, if divided by the amount of contributing cells yield *catchment averages* of these properties. Flow accumulation is initiated with a starting grid that contains the input values to be propagated until they meet the DEM boundaries or end in sinks. A *starting grid* that has the value of 1 everywhere will yield the amount of cells in the catchment or when multiplied with the cell size squared the TCA draining through each cell as the final value.

The starting grid may also consist of individual areas or starting zones from which values are propagated that may correspond to contaminants or mass movements and have a value of zero elsewhere. From this, the amount of contaminant or mass passed though a cell can be determined. The *downslope area* of a single starting zone is made up of all cells that have a nonzero value in the flow accumulation grid. The *upslope area* of a certain zone can be determined using upward flow directions.

The principle of flow accumulation is simple: when the draining proportions d out of one cell into its neighbours (must sum to 1) are known, also the receiving proportions r draining into one cell are known. The receiving proportions determine, which fractions of each neighbouring cell are received. The amount of mass

[5] For most applications $\Delta x = \Delta y$.

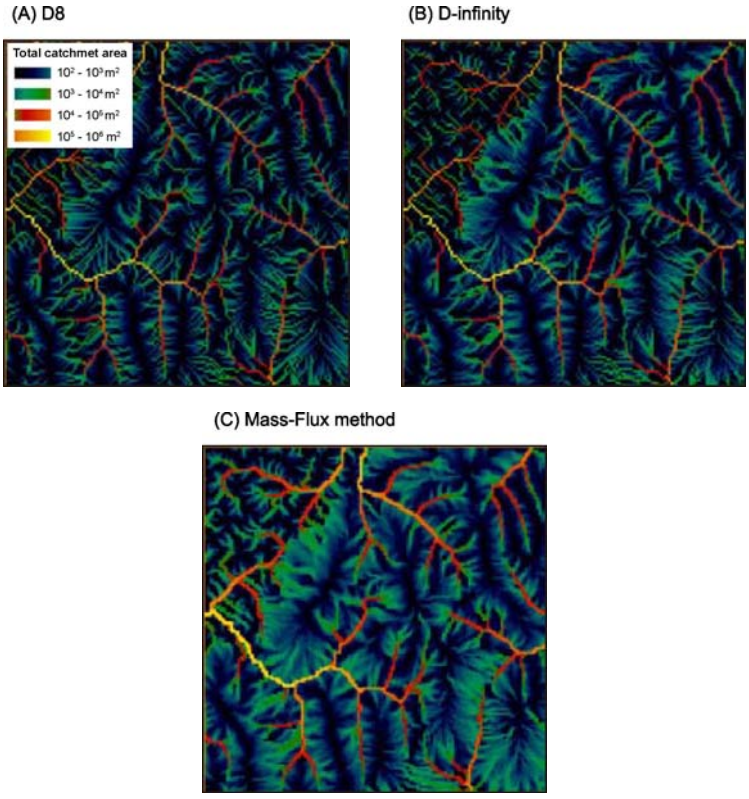

FIGURE 7 Total catchment area calculated for the Baranja Hill area using three different methods. (See page 713 in Colour Plate Section at the back of the book.)

(or volume, area or any other property) A that is accumulated in cell i is given by the sum of A in each neighbouring cell multiplied by the respective receiving fraction r plus the mass (or other quantity) input I in cell i itself:

$$A_i = \sum_{j=0}^{8} (A_{\mathrm{NB}j} \cdot r_{\mathrm{NB}j}) + I_i \tag{4.1}$$

Figures 7 and 8 show the spatial patterns resulting from the use of different flow direction methods for the calculation of TCA. D8 actually provides a very good estimate of the TCA for grid cells that are far enough downstream to be in the fully convergent, channelised portion of the landscape. However, for grid cells on hillslopes or near peaks and divides where the flow is divergent, values obtained by this method can be off by orders of magnitude. Especially here, in the hill slopes, the differences between the different approaches and between the values used for the dispersion coefficient in MFD are evident.

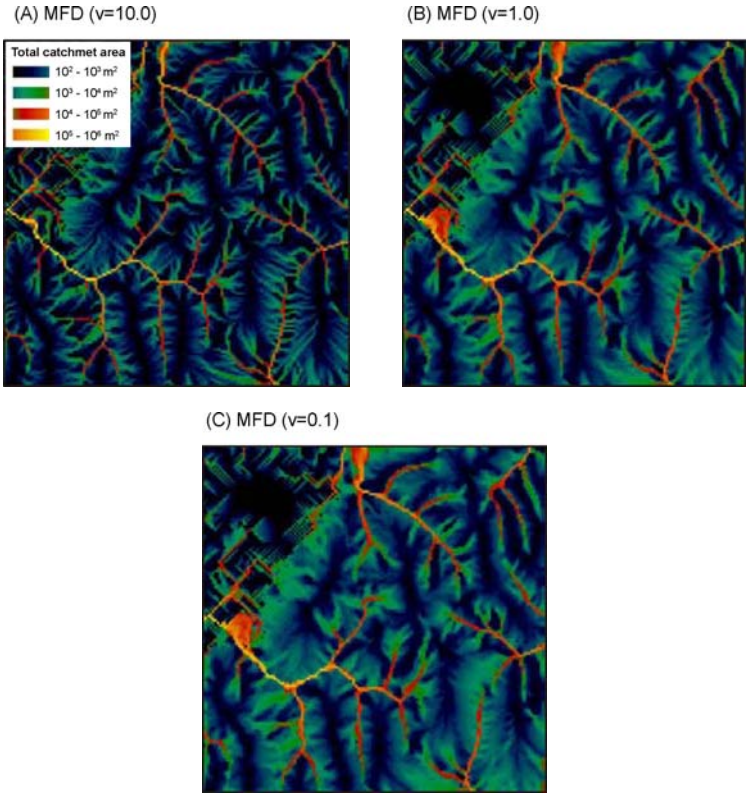

FIGURE 8 Total catchment area calculated for the Baranja Hill area using MFD and three different dispersion exponents. (See page 714 in Colour Plate Section at the back of the book.)

Figure 9 shows the result of applying D8, D-Infinity and MFM to the DEM of a cone. In parts (C) and (D), the MFM SCA grid shows a diamond pattern while the SCA grid is circular. Direct computation shows that a diamond pattern is the correct result — the area of each necktie-shaped polygon in Figure 6 is exactly the same.

In Figure 10 the propagation of one single mass input is displayed using different algorithms and different synthetic DEMs. The DEMs used are a sloping plane to show the handling of flow into a direction that is not a multiple of 45° and a sphere to demonstrate divergent flow.

> REMARK 4. *Calculation of catchment area or of accumulated terrain attributes based on catchment must be performed on DEMs that include the entire upslope area for all relevant pixels.*

Flow accumulation must be performed on the complete catchment of interest. The boundaries of the catchment should at least be one pixel away from the margin of the DEM to be sure of this. Otherwise, a contribution of unknown proportions is missing from the calculated results in the studied catchment. This edge contam-

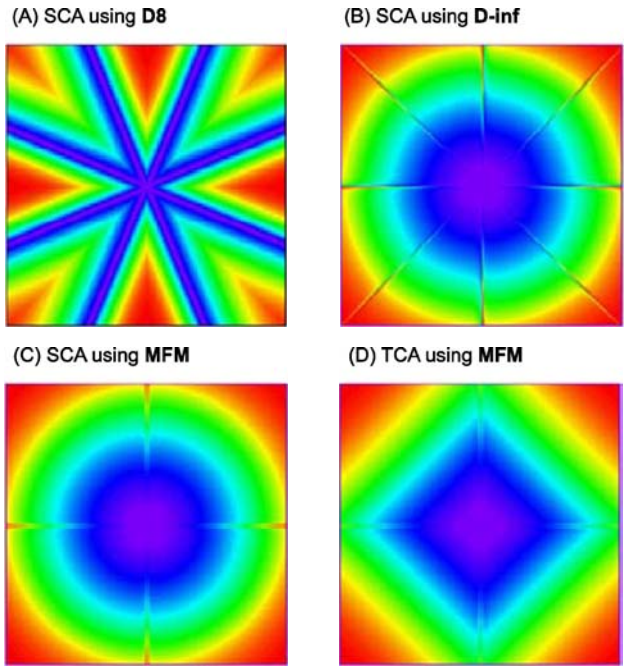

FIGURE 9 Parts (A)–(C) show the specific contributing area (SCA) calculated for the DEM of a cone sing D8, D-Infinity and MFM. The strong grid bias inherent in D8 is readily visible from the star pattern (A). Part (D) of this figure shows the total contributing area (TCA) calculated using MFM. This counter-intuitive result is correct because of the different flow widths of pixels (see Figure 6). When divided by the flow width, the SCA (C) shows the right circular pattern. (See page 715 in Colour Plate Section at the back of the book.) © 2005 Rivix LLC, used with permission.

ination effect can be assessed by propagating flow using a starting grid that only has a non-zero value in marginal pixels. All resulting pixels that have a value other than zero are affected by edge contamination and could thus contain an unknown error in their value of flow accumulation (Figure 11).

5. LAND-SURFACE PARAMETERS BASED ON CATCHMENT AREA

Catchment area is a powerful parameter of the amount of water draining though a cell that can be combined with other attributes to form compound indices. In the following we briefly describe the two most powerful and most frequently used indices: wetness and stream power.

The *Topographic Wetness Index*, also called Topographic Index or Compound Topographic Index (Quinn et al., 1991, 1995) is a parameter describing the tendency of a cell to accumulate water (Figure 12). The wetness index TWI is defined as:

$$\mathrm{TWI} = \ln\left[\frac{A}{\tan(\beta)}\right] \tag{5.1}$$

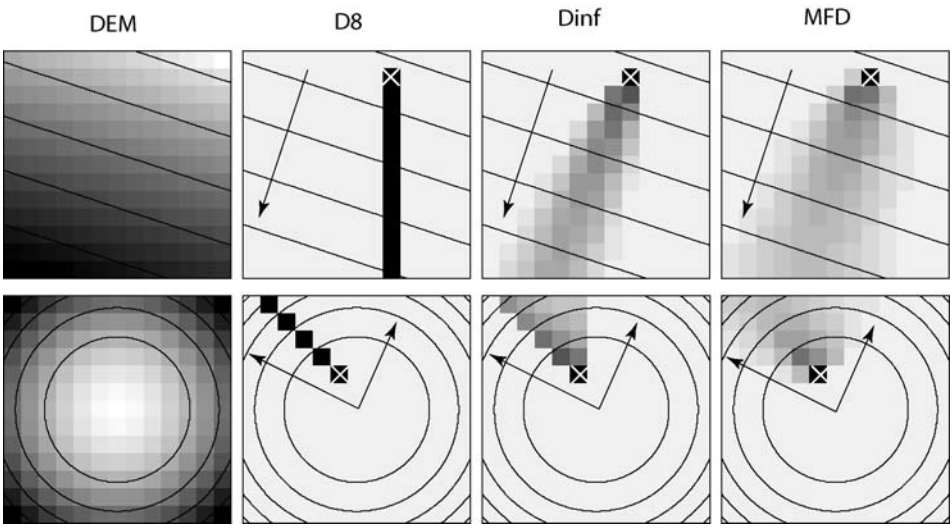

FIGURE 10 Graphic display of flow-propagation results using a synthetic DEMs (top: sloping plane, bottom: sphere). The first column (DEM) shows elevation values (dark: low, light: high) and isohypses. The remaining columns show topography by isohypses and arrows indicating the direction of drainage as well as grey values that correspond to the mass draining through one cell. In cells identified with a cross (starting zone), mass was inserted and propagated downwards. For D8, all downstream cells are black indicating that always the entire upstream mass was contained in the downstream cell. For D∞ and MFD, dispersion occurs and is indicated by grey cells where the upstream mass is divided into several downstream cells.

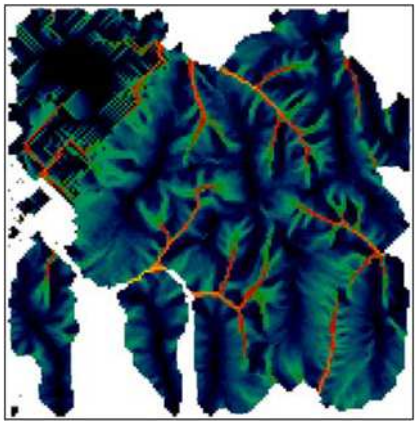

FIGURE 11 Edge-contaminated areas (white) have been removed from the calculated total contributing area. Both, the flow accumulation as well as the edge-contamination were computed using MFD. Other, less dispersive methods result in a smaller area of edge contamination. (See page 715 in Colour Plate Section at the back of the book.)

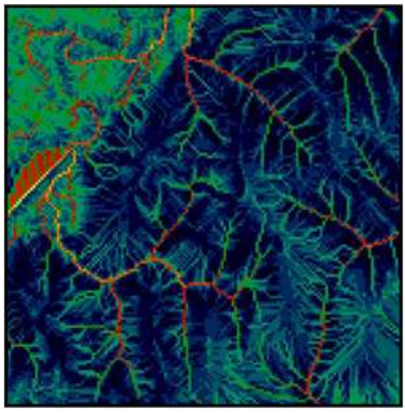

FIGURE 12 Wetness index calculated for the Baranja Hill. Values range from 3 (dark) to 20 (yellow); the data is linearly stretched. (See page 716 in Colour Plate Section at the back of the book.)

where A is the specific catchment area (SCA) and β is the local slope angle. It is based on a mass-balance consideration where the total catchment area is a parameter of the tendency to receive water and the local slope as well as the draining contour length (implicit in the specific catchment area) are parameters of the tendency to evacuate water. The TWI assumes steady-state conditions and spatially invariant conditions for infiltration and transmissivity. The natural logarithm scales this index to a more condensed and linear range. The original formulation also contained the lateral transmissivity of the soil profile that is usually omitted. This index is very powerful for a number of applications concerning vegetation, soil properties, landslide initiation and hydrology in hill slopes.

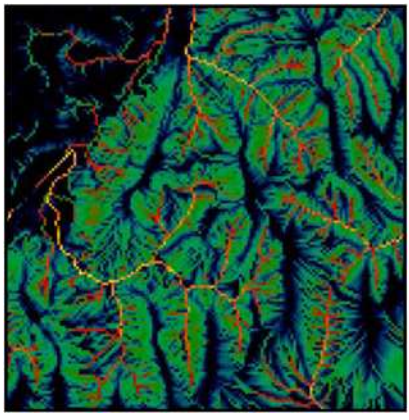

FIGURE 13 Stream power index calculated for the Baranja Hill. Values range from 1 (dark) to 12,000 (yellow); the data is stretched using logarithmic display. (See page 716 in Colour Plate Section at the back of the book.)

The *Stream Power Index* (Moore et al., 1988) can be used to describe potential flow erosion and related landscape processes (Figure 13). As specific catchment area and slope steepness increase, the amount of water contributed by upslope areas and the velocity of water flow increase, hence stream power and potential erosion increase. The stream power index SPI is defined as:

$$\mathrm{SPI} = A \cdot \tan(\beta) \tag{5.2}$$

A large number of other indices are proposed and discussed in the literature that use accumulated flow and relate to soil erosion (Moore and Burch, 1986) and landslide initiation (Montgomery and Dietrich, 1994). An overview and further discussion is provided by Moore et al. (1991a) and Wilson and Gallant (2000).

6. LAND-SURFACE OBJECTS BASED ON FLOW-VARIABLES

6.1 Drainage networks and channel attributes

One of the primary uses of the D8 method is the automated extraction of river network maps from raster DEMs. In addition to the map itself, a variety of attributes for each channel segment in a river network can be measured automatically. Figure 14 shows the *space-filling* drainage pattern that results from drawing a line segment between the centre of each grid cell and the neighbour grid cell that it flows towards, as determined by the D8 method. The drainage pattern is overlaid on an image which shows the locations of hills and valleys as resolved by the DEM.

Some grid cells are on hillslopes and some are in valleys. In order to create a map of the river network that drains this landscape, we need some method for *pruning* the dense drainage tree so that flow vectors on hillslopes are excluded. Many different pruning methods have been proposed, but no single method is best for all situations. A good pruning method should correctly identify the locations

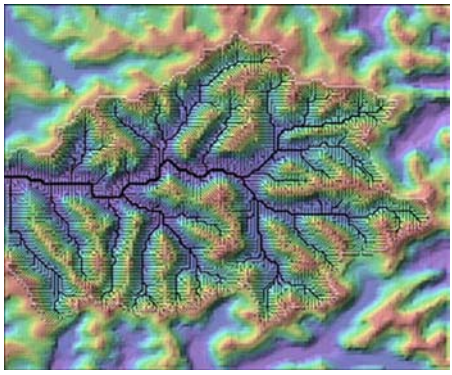

FIGURE 14 Complete drainage lines for one catchment. In the background, elevation is represented by colour. (See page 716 in Colour Plate Section at the back of the book.)

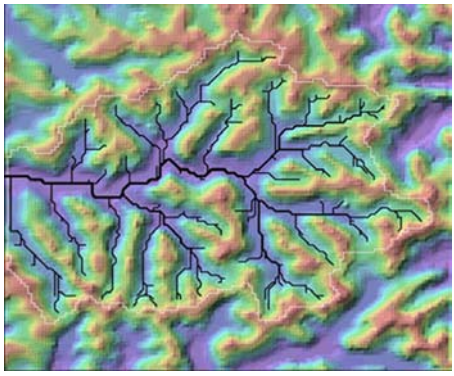

FIGURE 15 Drainage lines pruned by Horton–Strahler order. (See page 716 in Colour Plate Section at the back of the book.) © 2004 Rivix LLC, used with permission.

of channel sources as verified against a field survey. The most commonly-used pruning method is to first compute a grid of contributing areas (TCA) as explained in the previous section, and then remove the flow vector for any grid cell that has a TCA less than some specified threshold. A break in slope can often be identified in a scatter plot of slope versus area as explained by Tarboton et al. (1991) to identify this threshold. Sometimes, however, such a threshold is not apparent from the scatter plot.

Experience shows, however, that this simple method does not capture the natural variability that is present in real fluvial landscapes. The drainage density or degree of dissection is not spatially constant but varies with geology, elevation and other factors. A sometimes more robust method is to first create a grid of *Horton–Strahler order* for the dense drainage tree, and then remove flow vectors of grid cells that have orders less than some threshold value (Peckham, 1998), such as 3 (Figure 15).

> REMARK 5. *Land-surface objects most commonly extracted from DEMs are: river networks, ridge lines, slope breaks and watershed boundaries. These can be further analysed for numerous attributes and properties including: relative position, distances, attached areas/volumes, or density.*

Unlike the TCA method, this method automatically *adapts* to the variability of the landscape. Horton–Strahler order cannot increase from order 1 to order 2 until a streamline intersects another streamline, which means that it provides a simple measure of flow convergence. So whether a hillslope happens to be long or short, this method more accurately identifies the toe of the slope. In general, any grid of values can be used together with a threshold to differentiate hillslopes from channels. However, the grid values must increase (or decrease) downstream along every streamline or a disconnected network will result. This is what happens when we attempt to use a TCA (or SCA) grid from the D-Infinity or Mass-Flux Methods. Grids computed as a function of both contributing area and slope have

been proposed by Montgomery and Dietrich (1989, 1992) and others and appear to provide a process-based foundation for *source identification*.

Thresholds for network initiation work well in rugged terrain but produce spurious channels in flat areas (Tribe, 1992a). Once a pruning method has been applied to make a river network map, it is then possible to store the river network as an array of channel segments or links or Horton–Strahler streams, along with the network topology or connectedness and numerous attributes (Peckham, 1998).

Attributes can be computed for the channel segment itself, or for the basin that drains to its downstream end. Examples of attributes that can be computed and saved are: *upstream end pixel ID*, *downstream end pixel ID*, *stream order* (an integer-valued measure of stream hierarchy, Peckham and Gupta, 1999; Horton, 1932; Strahler, 1957), *contributing area* (above downstream end), *straight-line length*, *along-channel length*, *elevation drop*, *straight-line slope*, *along-channel slope*, *total length* (of all channels upstream), *Shreve magnitude* (total number of sources upstream of the pixel), *length of longest channel*, *relief*, *network diameter* (the maximum number of links between the pixel and any upstream source), *absolute sinuosity* (the ratio of the along-channel length and the straight-line length), *drainage density* (the ratio of the total length of drainage lines and the area drained by them, Horton, 1932; Tarboton et al., 1992; Dobos et al., 2005), *source density* (number of sources above the pixel divided by TCA), or *valley bottom flatness*.[6] Attributes for ensembles of sub-basins with the same Horton–Strahler order exhibit topological and statistical self-similarity. This property allows measurements at one scale to be extrapolated to other scales (Peckham, 1995a, 1995b; Peckham and Gupta, 1999).

6.2 Basin boundaries and attributes

D8 flow grids are also useful for extracting basin boundaries as polygons with associated attributes. Together, all of the grid cells that lie in the catchment of a given grid cell define a polygon. Numerous attributes, including its area, perimeter, diameter (the maximum distance between any two points on the boundary), mean elevation, mean slope and centroid coordinates can be computed. Many additional, flow-related attributes such as the maximum flow distance of any grid cell in the polygon to the outlet, or the total length of all channels within the polygon can also be computed.

The D8 method can also be used to partition a watershed into hydrologic subunits. Each subunit polygon represents the set of grid cells that contribute flow to a particular channel segment or reach. The set of subunit polygons fit together like puzzle pieces to completely cover the watershed. For exterior channel segments that terminate at sources, the polygons correspond to low-order sub-basins. For an interior channel segment, the polygon consists of two *wings*, one on each side of the segment, which often have a roughly triangular shape. Lumped hydrologic models can use these watershed subunits and their attributes to route flow through a watershed and compute *hydrographs* in response to storms. While

[6] An index computed as a multi-scale measure of flatness and lowness to identify depositional areas and valley bottoms (Gallant and Dowling, 2003).

lumped models are still in widespread use, spatially-distributed hydrologic models based on the D8 method (e.g. TopoFlow, Gridded Surface Subsurface Hydrologic Analysis — GSSHA) are starting to replace lumped models for many applications, and treat every grid cell as a control volume which conserves mass and momentum (see Chapter 25).

6.3 Flow distance, relief and longest channel length grids

D8 flow grids can be used to compute many other grid layers of hydrologic interest. One example is the along-channel *flow distance* from each grid cell to the edge of the DEM or to some other set of grid cells. A *relief grid* can also be defined, such that each grid cell is assigned a value as the difference between its own elevation and the highest elevation in the catchment that drains to it. Note that the relief of grid cells on drainage divides (peaks and ridges) is then simply zero. *Longest channel length* can also be computed as a grid layer, such that each grid cell is assigned a value as the length of the longest channel in the catchment that drains to it.

7. DEPOSITION FUNCTION

The concept of flow propagation is expanded by a deposition function to create a self-depleting flow that conserves mass between input and deposition in the *Mass Transport and Deposition* (MTD) algorithm (Gruber, 2007). This approach can be useful to model the re-distribution of eroded soil (Mitášová et al., 1996), the redistribution of snow by avalanches (Machguth et al., 2006) as well as other mass movements in steep topography (Chapter 23).

Similar concepts have also been applied to the delineation of lahar inundation zones (Iverson et al., 1998) and in the geomorphological model LAPSUS (Claessens et al., 2006; Schoorl et al., 2002). The key idea of the approach described here is that for each cell, a maximum deposition is pre-defined based on its slope (and possibly also other characteristics). During flow propagation, the flow though each cell is defined in a way similar to ordinary multiple flow direction methods and the local deposition is subtracted:

$$A_i = \sum_{j=0}^{8} (A_{\mathrm{NB}j} \cdot r_{\mathrm{NB}j}) + I_i - D_i \tag{7.1}$$

This means, that the flow passed though each cell A_i is equal to the sum of the flow received from its neighbours plus its own source term I_i, minus deposition D_i in this cell. Deposition D_i is limited by the amount of mass available $V_{\max}$ and the maximum deposition $D_{\max}$:

$$D_i = \min(D_{\max i}, V_{\max i}) \tag{7.2}$$

$$V_{\max i} = \sum_{j=0}^{8} (A_{\mathrm{NB}j} \cdot r_{\mathrm{NB}j}) + I_i \tag{7.3}$$

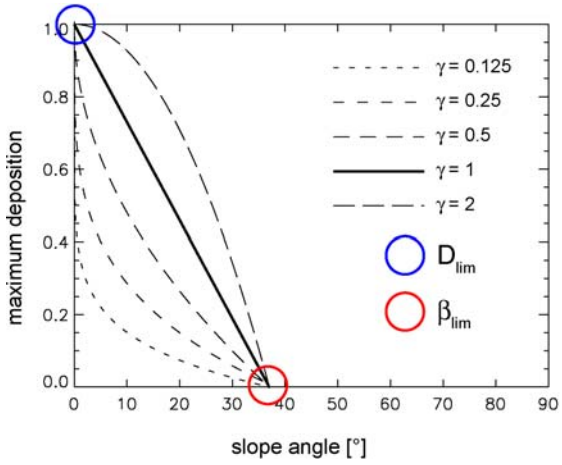

FIGURE 16 Maximum deposition as a function of slope.

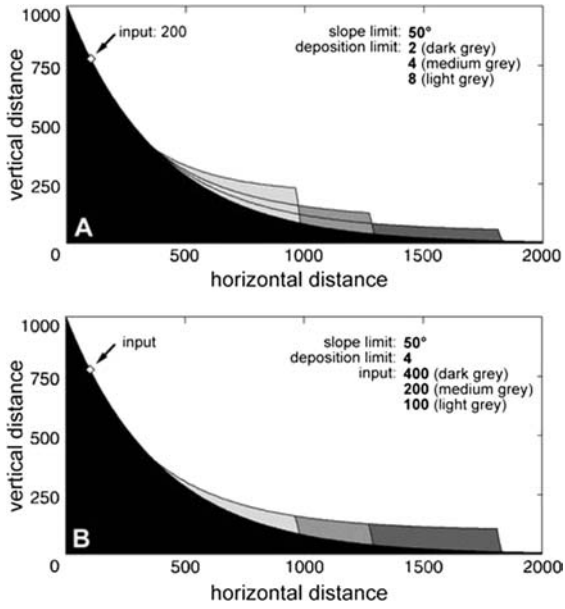

FIGURE 17 One-dimensional example of the influence that different deposition limits (A) and different amounts of mass input (B) have on the downslope deposition. Synthetic topography is black. Different deposits are shown in shades of grey. Reproduced from Gruber (2007) (see http://www.agu.org/pubs/copyright.html).

A generalised form of D_{max} can be described as a function of slope, e.g.:

$$D_{max} = \left[\left(1 - \left[\frac{\beta}{\beta_{lim}} \right]^{\gamma} \right) \geqslant 0 \right] \cdot D_{lim} \tag{7.4}$$

where β_{lim} is the slope limit below which deposition can take place, γ is an exponent controlling the relative emphasis of steep and gentle slopes and D_{lim} is the deposition limit that describes the maximum possible deposition in horizontal areas (Figure 16).

The maximum deposition can also be made dependent on curvature, surface cover or altered manually — a reservoir or other safety structures for instance may be large sinks for debris flows. Important in this concept is the pre-definition of D_{max} for each cell. Figure 17 illustrates the influence of D_{max} and different amounts of mass input on the deposition pattern in a one-dimensional example. Both influence the runout distance of the mass movement. Chapter 23 provides further illustration of the use of this approach.

8. FLOW MODELLING USING TIN-BASED ELEVATION MODELS

The use of gridded DEMs dominates most applications in environmental science due to the relative ease of their processing and their widespread availability. However, the use of TIN data has several distinct advantages over gridded data for applications such as landscape evolution modelling, hydrologic modelling or the derivation of flow related-variables. The main advantages of TINs over gridded DEMs are: variable spatial resolution and thus dramatic reduction of the number of elements in most cases; suitability for adaptive resampling of dense topographic fields according to point selection criteria (Lee, 1991; Kumler, 1994; Vivoni et al., 2004) that optimise the topographic or hydrologic significance and the size of the data set; the suitability for dynamic re-discretisation (e.g. in response to landscape evolution and the lateral displacement of landforms); the effective drainage direction is not restricted to multiples 45° and grid-bias in the statistics of derived variables is absent or less pronounced; suitability to re-projection without data loss; and the possibility to constrain data sets by streams or basin boundaries precisely as needed.

These advantages come at the price of an increased complexity of data structures and algorithms that needs to be handled in the development of methods in a TIN framework. A number of hydrology-related algorithms (e.g., for flow routing, network extraction, handling of sinks) exist for TINs (Preusser, 1984; Palacios-Velez and Cuevas-Renaud, 1986; Gandoy-Bernasconi and Palacios-Velez, 1990; Jones et al., 1990; Nelson et al., 1994; Tachikawa et al., 1994; Tucker et al., 2001; Vivoni et al., 2005) and contour lines (Moore et al., 1988). While many of them route flow along the edges of triangles, Tucker et al. (2001) propose a method that uses Voronoi polygons to approximate effective contour width between two neighbouring nodes and this permits the solution of diffusion-like equations.

9. SUMMARY POINTS

Elevation dominates the movement of water and a multitude of associated phenomena at or close to the land surface. Because of the wide availability of DEMs, geomorphometric techniques are outstandingly powerful in the quantification, analysis, forecasting or parametrisation of phenomena related to the flow of water on the Earth's surface. However, the choice of methods depends on the task at hand (e.g., stream hydrology in large basins or geomorphology in steep headwaters) and on the data available. In this chapter we have given an introduction to the most important concepts in geomorphometry that relate to the flow of water.

The methods explained represent a selection of methods originating from a large and active research community. Most parameters described in this chapter can be computed using software packages such as SAGA GIS (Chapter 12), RiverTools (Chapter 18), TAS (Chapter 16), GRASS (Chapter 17) or ArcGIS (Chapter 11).

IMPORTANT SOURCES

Wilson, J.P., Gallant, J.C. (Eds.), 2000. Terrain Analysis: Principles and Applications. Wiley, New York, 303 pp.

Peckham, S.D., 1998. Efficient extraction of river networks and hydrologic measurements from digital elevation data. In: Barndorff-Nielsen, O.E., et al. (Eds.), Stochastic Methods in Hydrology: Rain, Landforms and Floods. World Scientific, Singapore, pp. 173–203.

Tarboton, D.G., 1997. A new method for the determination of flow directions and upslope areas in grid digital elevation models. Water Resources Research 33 (2), 309–319.

Quinn, P., Beven, K., Chevallier, P., Planchon, O., 1991. The prediction of hillslope paths for distributed hydrological modeling using digital terrain models. Hydrological Processes 5, 59–79.

Moore, I.D., Grayson, R.B., Ladson, A.R., 1991a. Digital terrain modeling: a review of hydrological, geomorphological, and biological applications. Hydrological Processes 5 (1), 3–30.

O'Callaghan, J.F., Mark, D.M., 1984. The extraction of drainage networks from digital elevation data. Computer Vision, Graphics, and Image Processing 28, 323–344.